

Passive Control MHD Flow in the Presence of Arrhenius Chemical Reaction with Heat Generation/Absorption

Akindele M. Okedoye^{1,2}, Azeez A. Waheed³

¹Department of Mathematics, Covenant University, Ota, Ogun State, Nigeria

²Department of Mathematics, Federal University of Petroleum Resources, Effurun, Nigeria

³Department of Mathematics, Lead City University, Ibadan, Oyo State Nigeria

DOI: <https://doi.org/10.5281/zenodo.7503297>

Published Date: 04-January-2023

Abstract: The paper focuses on passive control MHD flow in the presence of Arrhenius Chemical reactions with Heat Generation Absorption. In this paper, a mathematical model for passive control MHD flow in the presence of Arrhenius Chemical reactions with Heat Generation Absorption was formulated. The momentum, energy, magnetic, and species equations were non-dimensionalized to arrive at dimensionless equations. The dimensionless equations were solved analytically with the use of asymptotic expansions defined about activation energy parameter ϵ . The properties of solutions were investigated for second order differential equations to show existence and uniqueness of solution of the problem. With graphical representation, the effect of various important physical parameters on velocity, energy, concentration and chemical species for reactivity parameter, convective heat transfer, heat generation, thermal buoyancy, Soret number and Eckert number were investigated. A table is also given that provides the results of different parameters on local Nusselt and Sherwood numbers. The passive control model reveals that the maximum velocity, temperature and concentration occurs at the surface which is dependent on the convective boundary conditions and convective heat transfer is seen to decline the chemical species distributions.

Keywords: Passive control, MHD, Chemical reactions, Heat Generation, Heat Transfer, Mass transfer, Exothermic Reactions, Boussinesq approximation, hydromagnetic.

I. INTRODUCTION

In several industrial manufacturing processes, including the flow along material handling conveyors, the cooling of an infinite metallic plate in a cooling bath, glass blowing, continuous casting, and fiber spinning, the flow due to a stretching surface also plays a role in the study of flow and, heat and mass transfer in the boundary layer induced by a surface moving with a uniform or non-uniform velocity in a quiescent ambient fluid. The investigation of boundary-layer behavior on continuously moving solid surfaces has caught the interest of various academics. Numerous processes, including the aerodynamic extrusion of plastic sheets and the boundary layer along a liquid film in condensation processes, Chamka [1], make use of the analysis of magneto-hydrodynamic (MHD) flows of electrically conducting fluid. According to Sajid & Hayat [2], the Prandtl number and radiation parameter have differing effects on the fluid's temperature on an exponentially stretched sheet. When Aliakbar et al. [3] investigated how thermal radiation affected the MHD flow of a Maxwellian fluid, they discovered that the fluid's temperature fell as the radiation parameter and Prandtl number increased. Additionally, it was discovered that the fluid's temperature increased as the Eckert number increased. Siddheshwar & Mahabaleswar [4] examined how heat and radiation sources affected the MHD flow of viscoelastic fluid across a stretching sheet in their study. Makinde and Sibanda took into account MHD mixed-convective flow and heat transfer past a vertical plate in a porous medium with constant wall suction in their work [5]. While Chamkha & Aly [6] focused on MHD free convection flow of a nanofluid via a vertical permeable plate in the presence of a heat source or sink, Aziz & Khan [7] examined the

natural convective boundary layer flow of nanofluid through a convectively heated vertical plate. Uddin et al [8] 's analysis of MHD free convective boundary layer flow over a flat vertical plate under Newtonian heating boundary conditions involved nanofluid research. Samad & Mansur-work Rahman's [9] examined the interaction between thermal radiation and unsteady MHD flow via a vertical porous plate. The plate was buried in a porous substance. While Md. Anwar Hossain & Munir [10] offered study of a 2-D mixed convection flow of viscous incompressible temperature dependent viscous fluid through a vertical plate, Makinde and Sibanda's study [5] concentrated on MHD mixed convective flow and heat transfer past a vertical plate submerged in a porous medium with continuous wall suction. While Fang [11] investigated how variations in fluid properties affect the boundary layers of a stretching surface, Mahmoud [12] showed how changing viscosity affects hydromagnetic boundary layer flow along a continuously rotating vertical plate sensitive to radiation. The free convection flow of a fluid with varying viscosity on a porous vertical plate is affected by radiation, according to M. Anwar Hossain et al research's [13]. When a transverse magnetic field was present, Poornima & Reddy [14] used a non-linear stretching sheet to generate sustained free convective boundary layer flow of a radiating nanofluid. Kandasamy et al. [15] investigated the effects of thermal stratification brought on by solar radiation, Brownian motion, and thermophoresis on the MHD boundary layer flow of nanofluid.

II. MATHEMATICAL FORMULATION

A. Governing equations

A number of physical issues, such as fluid undergoing exothermic or endothermic chemical reactions, make the study of heat generation or absorption impact in flowing fluids crucial. Chemical reactions occur between a foreign mass and the working fluid, which moves as a result of the stretching of a surface, in many chemical engineering processes. Several variables affect the chemical reaction's sequence. The first-order reaction, in which the rate of reaction is directly proportional to the species concentration, is one of the simplest chemical reactions. We believe that the inclusion of the magnetic field and the Arrhenius reaction would be intriguing and practical for applications in light of our steady-state study of the convection problem.

Consider the coupled heat and mass transfer through magnetohydrodynamics flow of a continuously moving vertical permeable surface in the presence of surface suction, transverse magnetic field effects, heat generation/absorption effects, and Arrhenius heat reactions.

The surface is kept at a constant temperature, the flow is supposed to be laminar and two-dimensional, and it is assumed that the flow will go on forever. Furthermore, it is believed that the applied transverse magnetic Reynolds number is low enough to ignore the induced magnetic field. The Hall effect, viscous dissipation, and Joule heating are also all ignored, and all thermophysical parameters are taken to be constant with the exception of the density in the buoyancy components of the momentum equation, which is approximated using the Boussinesq approximation.

With these presumptions, the steady equations that characterize the physical condition are as follows:

$$\frac{\partial v}{\partial y} = 0 \quad (1)$$

$$v \frac{\partial u}{\partial y} = \nu \frac{\partial^2 u}{\partial y^2} + g\beta_t(T - T_\infty) + g\beta_c(C - C_\infty) - \frac{\sigma B_0^2 u}{\rho} \quad (2)$$

$$\rho c_p v \frac{\partial T}{\partial y} = k \frac{\partial^2 T}{\partial y^2} + Q(T - T_\infty) + \mu \left(\frac{\partial u}{\partial y} \right)^2 \quad (3)$$

$$\rho \frac{\partial C}{\partial y} = D \frac{\partial^2 C}{\partial y^2} + k_r^2 (T - T_\infty)^r \exp\left(-\frac{E_a}{R_g T}\right) (C - C_\infty) \quad (4)$$

The appropriate physical boundary conditions for passive control involving slip and convective heat transfer could be written as follow:

$$u = L_1 \left(\frac{\partial u}{\partial y} \right), v = v_w, -k \frac{\partial T}{\partial y} = h[T - T_w], D_B \frac{\partial C}{\partial y} + \frac{D_T}{T_\infty} \frac{\partial T}{\partial y} = 0, \text{ at } y = 0 \left. \vphantom{u = L_1} \right\} \quad (5)$$

$$u \rightarrow U_\infty, T \rightarrow T_\infty, C \rightarrow C_\infty, \text{ as } y \rightarrow \infty,$$

where $u_w, v_0 > 0, T_w$ and C_w are surface speed, suction speed, surface temperature, and concentration, in that order.

B. Non - Dimensionalisation

From the continuity equation (1)

$$\frac{\partial v}{\partial y} = 0, \quad v(0) = v_w$$

Integrating we have the solution

$$v(y) = v_w \quad (6)$$

The momentum, energy, magnetic, and species equations (2-4) can be non-dimensionalized using the solution (6) by employing the subsequent non-dimensional variables.

$$y' = y \frac{v_w}{\nu}, u' = \frac{u}{u_w}, v' = \frac{v}{v_0}, L_1 = L_0 \frac{\nu}{v_w}, T - T_\infty = \frac{R_g T_\infty^2}{E_a} \theta, C - C_\infty = (C_w - C_\infty) \phi \quad (7)$$

After dropping primes ('), we have

$$\frac{d^2 u}{dy^2} + v_0 \frac{du}{dy} + Grt\theta + Grc\phi - Hu = 0 \quad (8)$$

$$\frac{d^2 \theta}{dy^2} + Pr v_0 \frac{d\theta}{dy} + Pr \beta \theta + \epsilon Ec \left(\frac{\partial u}{\partial y} \right)^2 = 0 \quad (9)$$

$$\frac{d^2 \phi}{dy^2} + Sc v_0 \frac{d\phi}{dy} + \epsilon \lambda \theta^r e^{\frac{\theta}{1+\epsilon\theta}} \phi = 0 \quad (10)$$

The dimensionless boundary conditions are

$$\left. \begin{aligned} u' = L_0 \left(\frac{\partial u'}{\partial y'} \right), -\frac{\partial \theta}{\partial y'} = Bi[\theta - 1], \frac{\partial \phi}{\partial y'} + Sr \frac{\partial \theta}{\partial y'} = 0, \text{ at } y' = 0 \\ u' \rightarrow \frac{U_\infty}{u_w}, \theta \rightarrow 0, \phi \rightarrow 0, \text{ as } y \rightarrow \infty, \end{aligned} \right\} \quad (11)$$

Where

$$\begin{aligned} \frac{\mu c_p}{k} = Pr, \frac{\mu}{D} = Sc, g\beta_t \frac{R_g T_\infty^2 \nu}{v_w^2 u_w E_a} = Grt, \frac{g\beta_c (C_w - C_\infty) \nu}{v_w^2 u_w} Grc, \frac{\sigma B_0^2 \nu}{v_w^2 \rho} = H, \frac{1}{Bi} = \frac{k v_w}{h \nu} \\ \frac{U_\infty}{u_w} = A, \frac{Q \nu^2}{v_w k} = Pr \beta, \frac{E_a^2 \mu}{R_g^2 T_\infty^3 k} u_w^2 = Ec, \frac{k_r^2 \nu^2}{D v_w^2 (C_w - C_\infty)} e^{-\frac{1}{\epsilon}} = \lambda, Sr = \epsilon \frac{D_T T_\infty}{D_B (C_w - C_\infty)} \end{aligned} \quad (12)$$

We assume exponential approximation similar to the one in Ayeni et. al [16], the polynomial approximation of the exponential term

$$\exp\left(\frac{\theta}{1+\epsilon\theta}\right) \approx 1 + \theta + \left(\frac{1}{2} - \epsilon\right) \theta^2$$

Then the equation (10) becomes

$$\frac{d^2 \phi}{dy^2} + Sc v_0 \frac{d\phi}{dy} + \epsilon \lambda \theta^r \left(1 + \theta + \left(\frac{1}{2} - \epsilon\right) \theta^2 \right) \phi = 0 \quad (13)$$

which has a quadratic temperature field.

The equivalent of the boundary condition becomes

$$\begin{aligned} u(0) = L_0 \frac{\partial u(y)}{\partial y} \Big|_{y=0}, \frac{\partial \theta(y)}{\partial y} \Big|_{y=0} = Bi(\theta(y) - 1) \Big|_{y=0}, \frac{\partial \phi(y)}{\partial y} + Sr \frac{\partial \theta(y)}{\partial y} \Big|_{y=0} = 0, \\ u \rightarrow 0, \theta \rightarrow 0, \phi \rightarrow 0, \text{ as } y \rightarrow \infty \end{aligned} \quad (14)$$

III. METHOD OF SOLUTION

Now, we consider the dimensionless equations (8), (9) and (13) with the boundary conditions (14). Using the asymptotic expansions defined about activation energy parameter ϵ , as

$$\left. \begin{aligned} u &\cong u_0 + \epsilon u_1 \\ \theta &\cong \theta_0 + \epsilon \theta_1 \\ \phi &\cong \phi_0 + \epsilon \phi_1 \end{aligned} \right\} \quad (15)$$

Substituting equation (15) into the dimensionless equations (8), (9) and (13) together with the boundary conditions (14) and separate the harmonic and non-harmonic respectively gives for zero order ϵ^0

$$\left. \begin{aligned} \frac{d^2}{dy^2} u_0(y) + v_0 \frac{d}{dy} u_0(y) + Grc\phi_0(y) + Grt\theta_0(y) - Hau_0(y) &= 0, \\ \frac{d^2}{dy^2} \theta_0(y) + Prv_0 \frac{d}{dy} \theta_0(y) + Pr\beta\theta_0(y) &= 0, \\ \frac{d^2}{dy^2} \phi_0(y) + Scv_0 \frac{d}{dy} \phi_0(y) &= 0. \end{aligned} \right\} \quad (16)$$

$$u_0 = L_0 \frac{\partial u_0}{\partial y}, \frac{\partial \theta_0}{\partial y} = Bi(\theta_0 - 1), \frac{\partial \phi_0}{\partial y} + Sr \frac{\partial \theta_0}{\partial y} = 0, u_0 \rightarrow A, \theta_0 \rightarrow 0, \phi_0 \rightarrow 0, \text{ as } y \rightarrow \infty \quad (17)$$

and for first order ϵ^1

$$\left. \begin{aligned} \frac{d^2}{dy^2} u_1(y) + v_0 \frac{d}{dy} u_1(y) + Grc\phi_1(y) + Grt\theta_1(y) - Hau_1(y) &= 0, \\ Prv_0 \frac{d}{dy} \theta_1(y) + Pr\beta\theta_1(y) + \frac{d^2}{dy^2} \theta_1(y) + Ec \left(\frac{d}{dy} u_0(y) \right)^2 &= 0 \\ \frac{d^2}{dy^2} \phi_1(y) + Scv_0 \frac{d}{dy} \phi_1(y) + \lambda\theta_0(y)r \left(1 + \theta_0(y) + \frac{1}{2}\theta_0(y)^2 \right) \phi_0(y) &= 0. \end{aligned} \right\} \quad (18)$$

$$u_1 = L_0 \frac{\partial u_1}{\partial y}, \frac{\partial \theta_1}{\partial y} = Bi\theta_1, \frac{\partial \phi_1}{\partial y} + Sr \frac{\partial \theta_1}{\partial y} = 0, u_1 \rightarrow 0, \theta_1 \rightarrow 0, \phi_1 \rightarrow 0, \text{ as } y \rightarrow \infty \quad (19)$$

The solutions approximated by equations (16) – (19) are obtained using method of undetermined coefficient and the result for zero order ϵ^0 are:

$$\left. \begin{aligned} \theta_0(y) &= a_1 e^{-my} \\ \phi_0(y) &= a_2 e^{-v_0 Scy}, \\ u_0(y) &= a_3 e^{-my} + a_4 e^{-v_0 Scy} + a_5 e^{-ny} \end{aligned} \right\} \quad (20)$$

While the first order solutions are:

$$\left. \begin{aligned} \theta_1(y) &= a_6 e^{-my} + a_7 e^{-2my} + a_8 e^{-(Scv_0+m)y} + a_9 e^{-(n+m)y} + (a_{10} + a_{12}) e^{-2Scv_0y} + a_{11} e^{-(Scv_0+n)y} \\ \phi_1(y) &= a_{14} e^{-(v_0 Sc+m(r+2))y} + a_{15} e^{-(v_0 Sc+m(r+1))y} + a_{16} e^{-(v_0 Sc+mr)y} + a_{17} e^{-v_0 Scy} \\ u_1(y) &= a_{18} e^{-ny} + a_{19} e^{-my} + a_{20} e^{-2my} + a_{21} e^{-(Scv_0+m)y} + a_{22} e^{-(n+m)y} + a_{23} e^{-2v_0 Scy} + a_{24} e^{-(Scv_0+n)y} \\ &\quad + a_{26} e^{-(Scv_0+m(r+2))y} + a_{27} e^{-(Scv_0+m(r+1))y} + a_{28} e^{-(Scv_0+mr)y} + a_{28} e^{-(Scv_0+mr)y} \end{aligned} \right\} \quad (21)$$

Solution for order of $\epsilon^i, i \geq 2$ are negligible.

Using equations (20) and (21) in equation (15), we have the solutions for velocity, temperature and species concentrations, respectively as

$$\begin{aligned} u(y) &\cong a_3 e^{-my} + a_4 e^{-v_0 Scy} + a_5 e^{-ny} + \epsilon (a_{18} e^{-ny} + a_{19} e^{-my} + a_{20} e^{-2my} + a_{24} e^{-(Scv_0+n)y} \\ &\quad + a_{21} e^{-(Scv_0+m)y} + a_{22} e^{-(n+m)y} + a_{23} e^{-2v_0 Scy} + a_{26} e^{-(Scv_0+m(r+2))y} \\ &\quad + a_{27} e^{-(Scv_0+m(r+1))y} + a_{28} e^{-(Scv_0+mr)y} + a_{28} e^{-(Scv_0+mr)y} \end{aligned} \quad (22)$$

$$\phi(y) \cong a_2 e^{-v_0 S c y} + \epsilon (a_{14} e^{-(v_0 S c + m(r+2))y} + a_{15} e^{-(v_0 S c + m(r+1))y} + a_{16} e^{-(v_0 S c + m r)y} + a_{17} e^{-v_0 S c y}) \quad (23)$$

$$\theta(y) \cong a_1 e^{-m y} + \epsilon (a_6 e^{-m y} + a_7 e^{-2m y} + a_8 e^{-(S c v_0 + m)y} + a_9 e^{-(n+m)y} + (a_{10} + a_{12}) e^{-2S c v_0 y} + a_{11} e^{-(S c v_0 + n)y}) \quad (24)$$

All parameters are as define in the appendix.

A. Rate of Heat and Mass Transfer at the wall

Local Skin-Friction τ , Nusselt number Nu , and Sherwood number Sh are the quantities of relevance to engineers. Following Mohamed et al. [17] definition, these numbers are:

$$\tau = \frac{\tau_w}{\rho_{nf} U_w^2}, \quad Nu_x = \frac{E_a q_w}{k R_g T_\infty^2}, \quad Sh_x = \frac{x q_m}{D_B (C_w - C_\infty)} \quad (25)$$

where τ_w represents the skin friction along the surface, q_w the heat flux from the surface and are respectively given as

$$\tau_w = \left[v \frac{\partial u}{\partial y} \right]_{y=0}, \quad q_w = \left[-k \frac{\partial T}{\partial y} \right]_{y=0}, \quad q_m = \left[-D \frac{\partial C}{\partial y} \right]_{y=0} \quad (26)$$

where q_w and q_m , represents the heat and mass fluxes at the surface respectively.

Using similarity transformation, we have

$$\tau = \frac{du}{dy} \Big|_{y=0}, \quad Nu = - \frac{d\theta}{dy} \Big|_{y=0}, \quad Sh = \frac{d\phi}{dy} \Big|_{y=0} \quad (27)$$

Using equations (22), (23) and (24) in equation (27), the dimensionless flow rate function at the boundary becomes

$$\tau = -a_3 m - a_4 S c v_0 - a_5 n - \epsilon (a_{18} n + a_{19} m + 2a_{20} m + a_{21} (S c v_0 + m) + a_{22} (n + m) + 2a_{23} S c v_0 + a_{24} (S c v_0 + n) + a_{26} (S c v_0 + m(r + 2)) + a_{27} (S c v_0 + m(r + 1)) + a_{28} (S c v_0 + m r) + a_{29} S c v_0) \quad (28)$$

$$Nu = a_1 m + \epsilon (a_6 m + 2a_7 m + a_8 (S c v_0 + m) + a_9 (n + m) + 2(a_{10} + a_{12}) S c v_0 + a_{11} (S c v_0 + n)) \quad (29)$$

$$Sh = a_2 S c v_0 + \epsilon (a_{14} (S c v_0 + m(r + 2)) + a_{15} (S c v_0 + m(r + 1)) + a_{16} (S c v_0 + m r) + a_{17} S c v_0) \quad (30)$$

IV. RESULTS AND DISCUSSIONS

A. Condition for Existence of Solution

It should be noted here that the above solutions will be unique and real, if and only if the following conditions hold:

$$m = \frac{1}{2} \left(P r v_0 + \sqrt{P r^2 v_0^2 - 4 P r \beta} \right) \in \mathbb{R}, \quad n = \frac{1}{2} \left(v[0] + \sqrt{v_0^2 - 4 H} \right) \in \mathbb{R}$$

$$P r^2 v_0^2 - 4 P r \beta \geq 0, \quad v_0^2 - 4 H \geq 0$$

Which implies that

$$\beta \leq \frac{P r v_0^2}{4}, \quad H \leq \frac{v_0^2}{4}$$

But for plasma, which is the supposed fluid under consideration, $P r = 0.71$, thus

$$\beta \leq \frac{0.71 v_0^2}{4} = 0.177 v_0^2$$

Typical values for β suggested by $v_0 > 0$ when ϵ is taken to be 0.1 is depicted in Figure 2.

Lemma. Let $G r t > 0, G r c > 0, H > 0, v_0 > 0, \lambda \in [-a, a], r, a \in \mathcal{R}^+$. Then $\varphi(y), \varphi(y) = u(y), \theta(y), \phi(y)$ has no maximum in the entire domain of the flow process.

Proof.

From equations (21) – (23) we obtain

$$\begin{aligned} \frac{d}{dy}\theta(y) = & -ma_1e^{-my} - \epsilon(ma_6e^{-my} + 2ma_7e^{-2my} + (Scv_0 + m)a_8e^{-(Scv_0+m)y} \\ & + (n + m)a_9e^{-(n+m)y} + 2Scv_0(a_{10} + a_{12})e^{-2Scv_0y} + (Scv_0 + n)a_{11}e^{-(Scv_0+n)y}) \end{aligned} \quad (31)$$

$$\begin{aligned} \frac{d}{dy}\phi(y) = & -v_0Sca_2e^{-v_0Scy} - \epsilon\left((v_0Sc + m(r + 2)) + a_{14}e^{-(v_0Sc+m(r+2))y} \right. \\ & \left. + (v_0Sc + m(r + 1))a_{15}e^{-(v_0Sc+m(r+1))y} + (v_0Sc + mr)a_{16}e^{-(v_0Sc+mr)y} + v_0Sca_{17}e^{-v_0Scy}\right) \end{aligned} \quad (32)$$

$$\begin{aligned} \frac{d}{dy}u(y) = & -ma_3e^{-my} - v_0Sca_4e^{-v_0Scy} - na_5e^{-ny} - \epsilon(na_{18}e^{-ny} + ma_{19}e^{-my} + 2ma_{20}e^{-2my} \\ & + (Scv_0 + m)a_{21}e^{-(Scv_0+m)y} + (n + m)a_{22}e^{-(n+m)y} + 2v_0Sca_{23}e^{-2v_0Scy} \\ & + (Scv_0 + m(r + 2))a_{26}e^{-(Scv_0+m(r+2))y} + (Scv_0 + n)a_{24}e^{-(Scv_0+n)y} \\ & + (Scv_0 + mr)a_{28}e^{-(Scv_0+mr)y} + (Scv_0 + m(r + 1))a_{27}e^{-(Scv_0+m(r+1))y}) \end{aligned} \quad (33)$$

We let

$$e^{-my} = x_1, e^{-v_0Scy} = x_2, e^{-ny} = x_3,$$

And set

$$\frac{d}{dy}\varphi(y) = 0, \text{ where } \varphi = u, \theta, \phi$$

We have

$$\begin{aligned} -ma_1x_1 - \epsilon(ma_6x_1 + 2ma_7x_1^2 + (Scv_0 + m)a_8x_1x_2 \\ + (n + m)a_9x_1x_2 + 2Scv_0(a_{10} + a_{12})x_1^2 + (Scv_0 + n)a_{11}x_2x_3) = 0 \end{aligned} \quad (34)$$

$$\begin{aligned} -v_0Sca_2x_2 - \epsilon\left((v_0Sc + m(r + 2))a_{14}x_1^3x_2 \right. \\ \left. + (v_0Sc + m(r + 1))a_{15}x_1^2x_2 + (v_0Sc + mr)a_{16}x_1x_2 + v_0Sca_{17}x_2\right) = 0 \end{aligned} \quad (35)$$

$$\begin{aligned} -ma_3x_1 - v_0Sca_4x_2 - na_5x_3 - \epsilon(na_{18}x_3 + ma_{19}x_1 + 2ma_{20}x_1^2 \\ + (Scv_0 + m)a_{21}x_1x_2 + (n + m)a_{22}x_1x_3 + 2v_0Sca_{23}x_2^2 + (Scv_0 + n)a_{24}x_2x_3 \\ + (Scv_0 + m(r + 2))a_{26}x_1^3x_2 + (Scv_0 + m(r + 1))a_{27}x_1^2x_2 + (Scv_0 + mr)a_{28}x_1x_2) = 0 \end{aligned} \quad (36)$$

respectively.

On solving for x_1, x_2 and x_3 , the two real roots are

$$x_1 = 0, x_2 = 0, x_3 = 0 \quad (37)$$

$$x_1 = -\frac{1}{2} \frac{m(\epsilon a_6 + a_1)}{\epsilon(Scv_0(a_{10} + a_{12}) + ma_7)}, x_2 = 0, x_3 = \frac{1}{2} \frac{a_3^2 m(\epsilon a_6 + a_1)}{\epsilon(Scv_0(a_{10} + a_{12}) + ma_7)a_5 n} \quad (38)$$

But

$$y = -\frac{1}{m} \ln x_1 = -\frac{1}{v_0Sc} \ln x_2 = -\frac{1}{n} \ln x_3 < 0$$

Thus, by the condition of the theorem, position y at which a maximum occur does not exist.

Hence the theorem!

Corollary: As consequence of the above, the maximum velocity, temperature and concentration occurs at the surface which is dependent on the convective boundary conditions.

B. Discussion of Results

In respect to the surface suction/injection, Figure 2 shows the link between the heat generation/absorption parameter and Hartman number. Hartman number and the heat generation/absorption parameter both appear to behave similarly within the boundary, with the Lorentz force increasing more quickly than the heat generation/absorption parameter in relation to an increase in suction/injection.

Figures 3 and 4 shows the effect of Lorentz force, heat generation/absorption and convective heat transfer on the velocity respectively. From the figures we observe that the Lorentz force in term of Hartman and heat generation/absorption decline the bulk velocity of the flow field with maximum velocity at the surface depending on the slip factor. In Figure 5-12, we display the impact of and convective heat transfer, Eckert number, velocity slip factor, chemical reactivity parameter, mass and thermal buoyancy, Frank Kamnetski parameter and, Soret number respectively on velocity distribution. From the figures, it was discovered that an increase in each parameter resulted in increase in velocity of the flow field.

Table 1: Effect of governing parameters on Velocity, Temperature and Concentration initial values and flow rate at the wall.

	$u(0)$	$\theta(0)$	$\phi(0)$	τ	Nu	Sh
$H = 0.39$	13.91	0.20	1.09	-22.91775	0.15985	-0.36733
$H = 0.40$	4.23	0.20	1.14	-7.05459	0.15985	-0.41557
$H = 0.55$	1.04	0.20	-1.78	-1.59139	0.15994	2.11514
$H = 0.56$	0.40	0.20	-1.04	-0.43785	0.15995	1.41483
$\beta = 0.30$	13.91	0.10	-0.79	-22.91775	0.18013	-0.85336
$\beta = 0.31$	6.38	0.12	-0.66	-10.56172	0.17684	-0.57965
$\beta = 0.32$	3.51	0.13	-0.39	-5.86389	0.17384	-0.37377
$\beta = 0.35$	1.65	0.15	-0.35	-2.80381	0.16982	-0.32697
$Ec = 0.05$	3.50	0.20	-0.37	-5.86305	0.15974	-0.35666
$Ec = 0.10$	6.97	0.24	-0.39	-11.54795	0.15618	-0.39337
$Ec = 0.20$	13.91	0.28	-0.44	-22.91775	0.15244	-0.46678
$Ec = 0.50$	34.73	0.40	-0.58	-57.02714	0.14121	-0.68702
$\lambda = 00.0$	13.85	0.20	-0.49	-22.82995	0.15985	-0.43810
$\lambda = 10.0$	17.91	0.20	-0.40	-28.68314	0.15985	-0.36905
$\lambda = 25.0$	23.99	0.20	-0.31	-37.46293	0.15985	-0.30001
$\lambda = 50.0$	34.12	0.20	-0.22	-52.09592	0.15985	-0.23097
$Grc = 1.0$	2.80	0.20	-0.35	-4.36716	0.15991	-0.32138
$Grc = 3.0$	8.36	0.20	-0.35	-13.63661	0.15992	-0.32591
$Grc = 5.0$	13.91	0.20	-0.37	-22.91775	0.15985	-0.33464
$Grc = 7.0$	19.42	0.20	-0.36	-32.15353	0.15970	-0.34756
$Grt = 0.8$	0.45	-0.36	-0.36	-1.17358	0.04074	-0.33976
$Grt = 1.0$	0.78	-2.05	-0.64	-1.68605	-0.33850	-0.45883
$Grt = 1.5$	1.89	-4.87	-1.57	-3.46131	-0.97802	-0.81539
$Grt = 2.0$	3.44	-8.82	-5.35	-5.94226	-1.87784	-2.22087
$Bi = 0.8$	87.50	0.50	-0.92	-143.52394	0.39836	-0.89110
$Bi = 0.4$	38.76	0.34	-0.60	-63.68401	0.26611	-0.57392
$Bi = 0.2$	13.91	0.20	-0.35	-22.91775	0.15985	-0.33464
$Bi = 0.1$	4.28	0.11	-0.19	-7.08649	0.08885	-0.18230
$L_0 = 0.0$	10.98	0.20	-0.35	-19.62632	0.15986	-0.33492
$L_0 = 0.5$	15.87	0.20	-0.35	-25.12046	0.15985	-0.33482
$L_0 = 1.0$	20.78	0.20	-0.35	-30.64089	0.15986	-0.33471

$L_0 = 2.0$	30.62	0.20	-0.35	-41.70547	0.15985	-0.33447
$\epsilon = 0.01$	1.37	0.20	-0.34	-2.37309	0.15992	-0.32133
$\epsilon = 0.02$	2.76	0.20	-0.36	-4.65583	0.15978	-0.34942
$\epsilon = 0.03$	4.15	0.20	-0.37	-6.93857	0.15970	-0.36421
$\epsilon = 0.05$	6.94	0.20	-0.39	-11.50405	0.15955	-0.39378
$Sr = 0.5$	3.49	0.20	-0.09	-5.52326	0.15991	-0.08043
$Sr = 1.0$	6.97	0.20	-0.17	-11.31593	0.15992	-0.16219
$Sr = 2.0$	13.91	0.20	-0.35	-22.91775	0.15985	-0.33464
$Sr = 4.0$	27.50	0.20	-0.76	-45.79743	0.15933	-0.74962
$Pr = 0.01$	0.40	0.46	-0.24	1.57435	0.10630	-0.22030
$Pr = 0.03$	0.17	0.33	-0.29	0.60079	0.13440	-0.27542
$Pr = 0.71$	-0.11	0.07	-0.39	-0.07327	0.18509	-0.35593
$Pr = 2.36$	-0.11	0.03	-0.41	-0.31929	0.19313	-0.38411

The impact of heat generation, Eckert number and convective heat transfer is displayed in Figures 13-15 respectively. As expected, as much heat is generated, the bulk available heat in the flow system decrease resulting into lowering of temperature in the flow field while, Eckert number which expresses the relationship between the flow kinetic energy and the boundary enthalpy difference is seen to lower the flow temperature as a result of the irreversible process that took place in the system. As convective heat transfer increases, the temperature of the flow field increases with maximum temperature only at the surface. While we show in Figure 16 that increase in thermal buoyancy increase the ability of the flow to withstand heat and thereby encouraging the motion of plate in the direction of the flow.

Figures 17-22 depict the chemical concentration species relative to changes in reactivity parameter, convective heat transfer, heat generation, thermal buoyancy, Soret and Eckert numbers respectively. These figures show that the reaction flow is a destructive one with more species consumed as destructive parameter increases and vice versa as shown in Figure 17. The convective heat transfer is seen to decline the chemical species distributions as displayed in Figure 18. While Figure 19 indicates that more chemical species is consumed with increase in heat generation. Increase in thermal buoyancy Soret and Eckert numbers consumed more chemical species as displayed in Figures 20, 21 and 22 respectively.

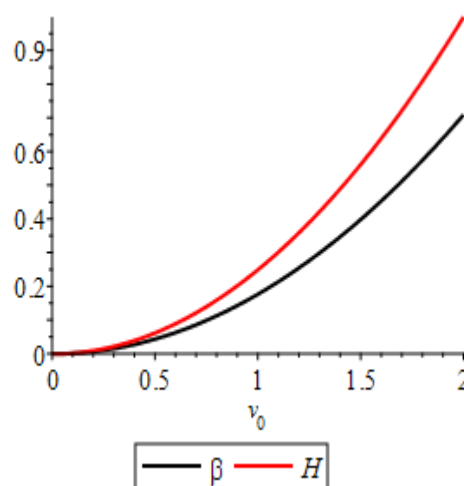


Figure 2: Relationship between β , H and v_0

The variation of flow governing parameters on the rate of flow at the wall in terms of Skin Friction, Nusselt number and Sherwood number representing aerodynamics or hydrodynamic drag, rate of heat transfer at the wall and rate of mass transfer at the wall respectively. It should be pointed out that Skin-Friction is a resistant force exerted on an object passing through the fluid. This type of force is caused by the fluid viscosity which is developed from laminar to turbulent drag as object passes through the fluid and vice versa. In Table 1, we depict the effect of the various parameters on the flow rate at the wall and the resultant effect is clearly shown in the table.

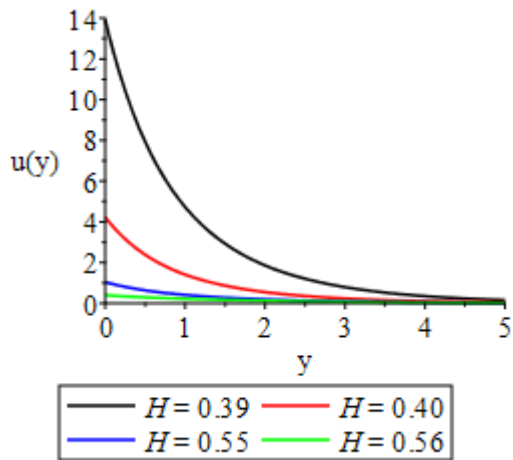


Figure 3: Velocity Distributions for various values of Hartman number

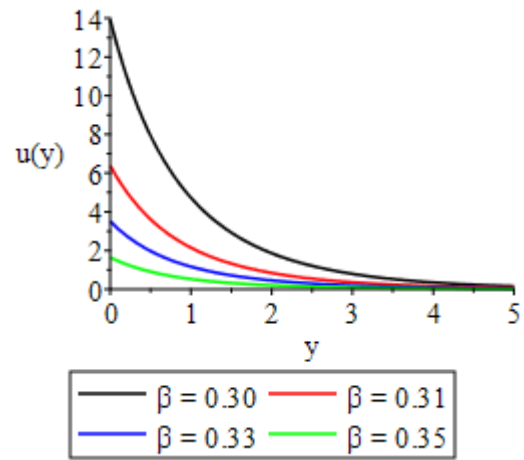


Figure 4: Velocity Distributions for various values of heat generation/absorption

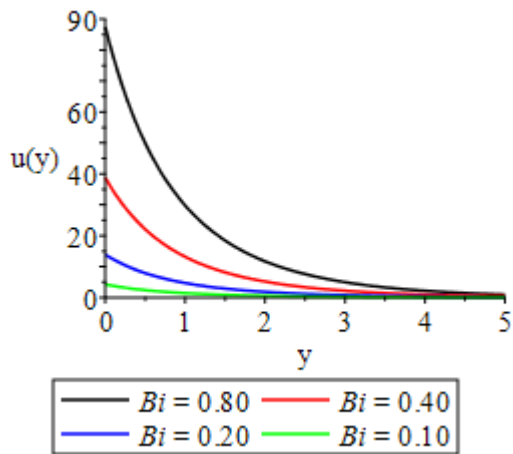


Figure 5: Velocity Distributions for various values of Convective heat transfer

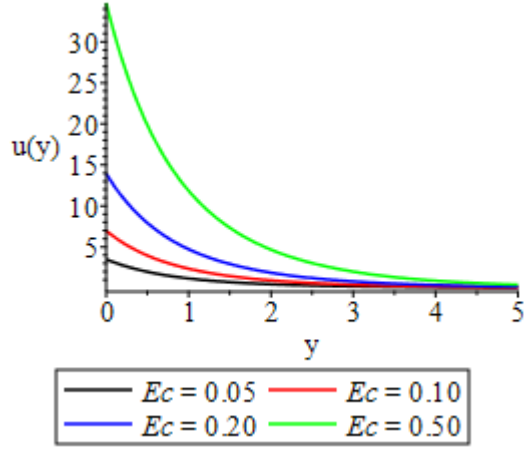


Figure 6: Velocity Distributions for various values of Eckert number

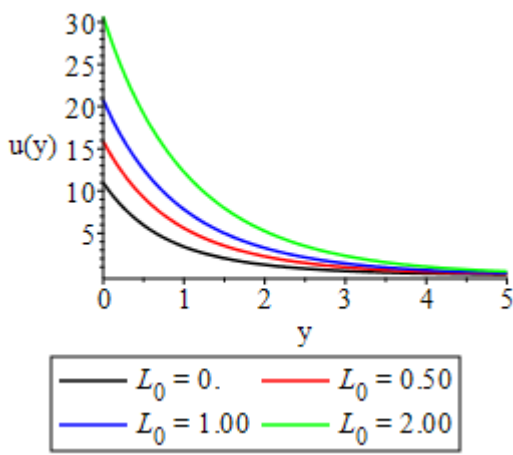


Figure 7: Velocity Distributions for various values of velocity slip factor

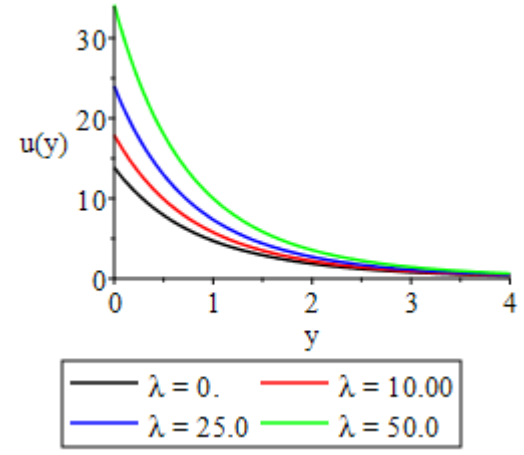


Figure 8: Velocity Distributions for various values of reactivity parameter

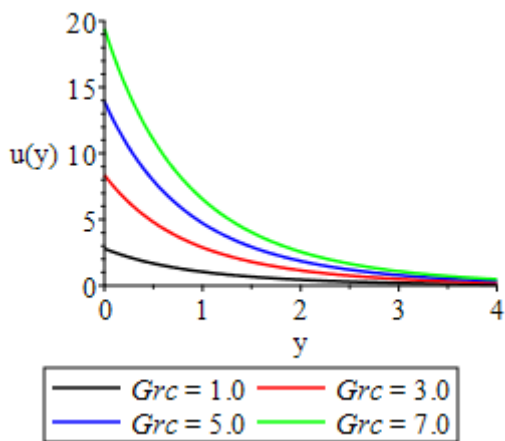


Figure 9: Velocity Distributions for various values of mass buoyancy

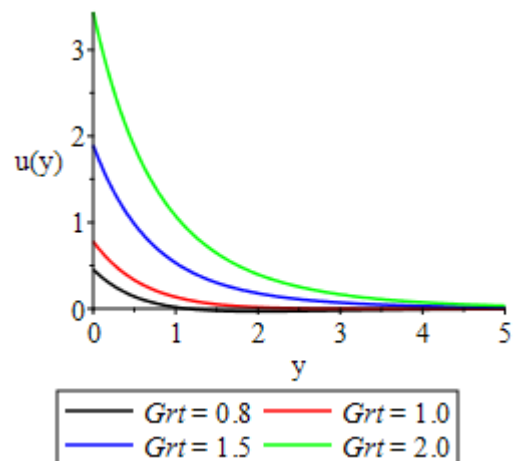


Figure 10: Velocity Distributions for various values of thermal buoyancy

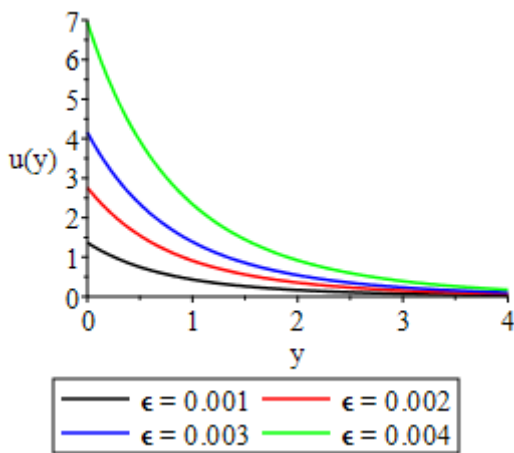


Figure 11: Velocity Distributions for various values of Frank Kamnitski parameter

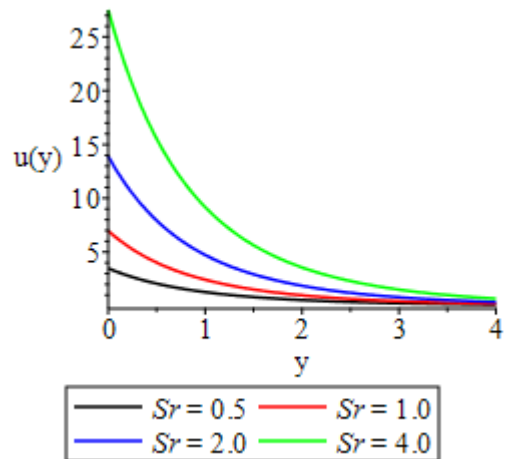


Figure 12: Velocity Distributions for various values of Soret number

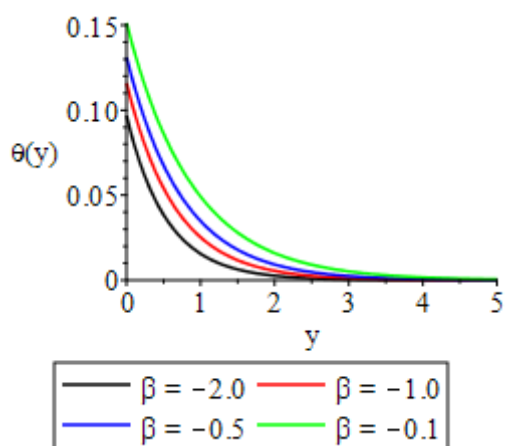


Figure 13: Temperature Distributions for various values of heat generation/absorption

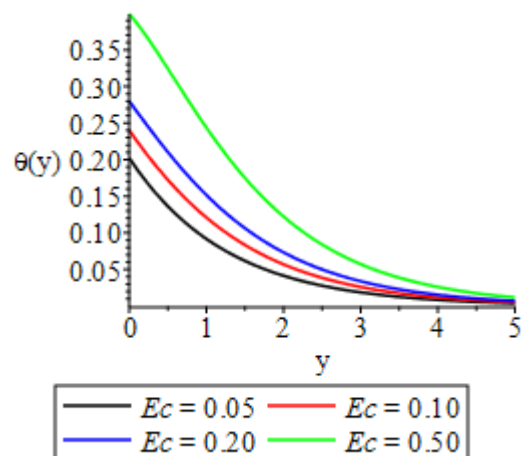


Figure 14: Temperature Distributions for various values of Eckert number

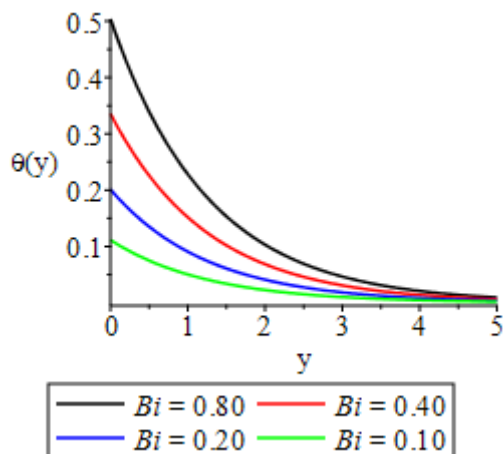


Figure 15: Temperature Distributions for various values of convective heat transfer

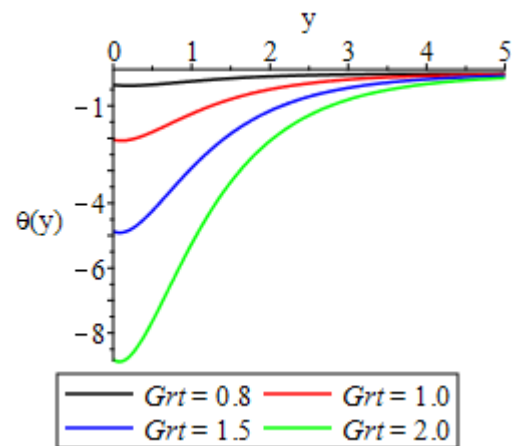


Figure 16: Temperature Distributions for various values of thermal buoyancy

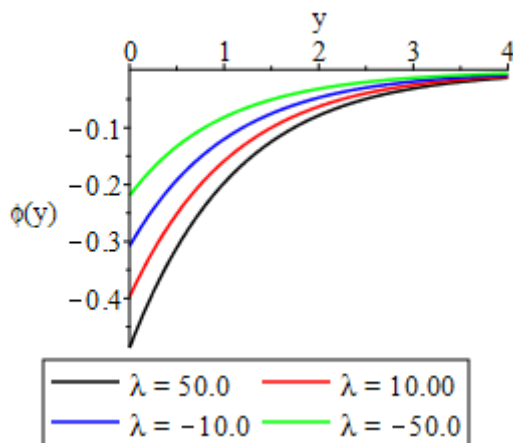


Figure 17: Chemical Species Distributions for various values of reactivity parameter

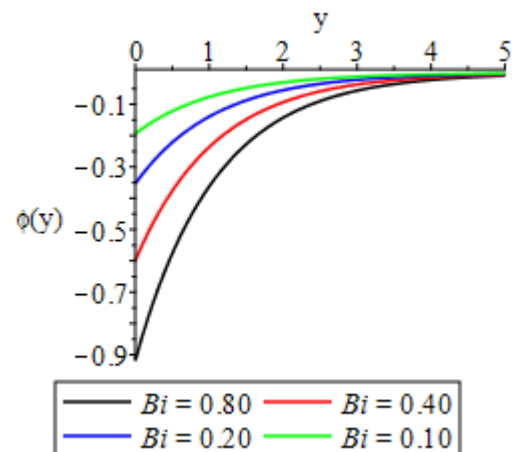


Figure 18: Chemical Species Distributions for various values of convective heat transfer

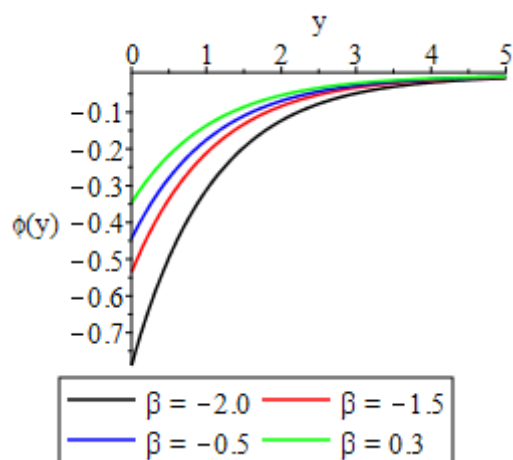


Figure 19: Chemical Species Distributions for various values of heat generation

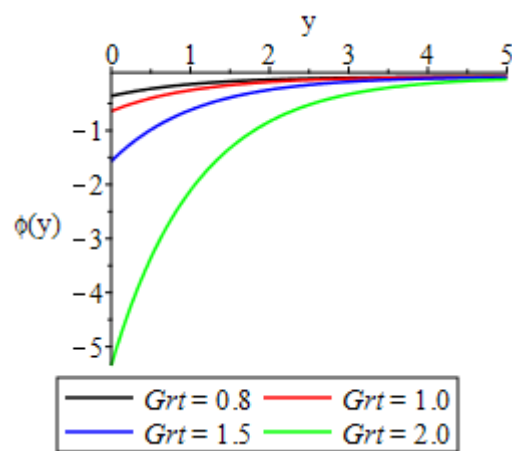


Figure 20: Chemical Species Distributions for various values of thermal buoyancy

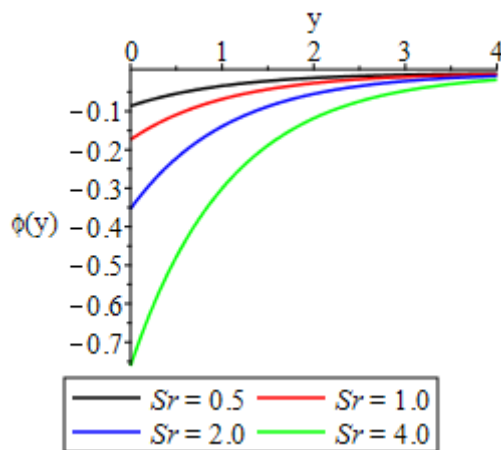


Figure 21: Chemical Species Distributions for various values of Soret number

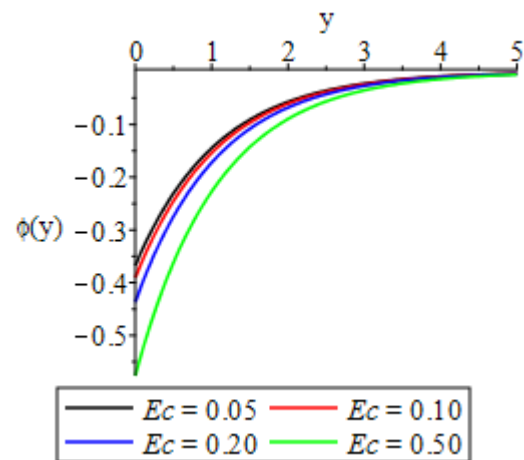


Figure 22: Chemical Species Distributions for various values of Eckert number

V. CONCLUDING REMARK

From the both the analytical and graphical solutions obtained, we deduced the following:

- the maximum velocity, temperature and concentration occurs at the surface which is dependent on the convective boundary conditions
- the Lorentz force and heat generation/absorption decline the bulk velocity of the flow field
- convective heat transfer, Eckert number, velocity slip factor, chemical reactivity parameter, mass and thermal buoyancy, Frank Kamnitski parameter and, Soret number respectively in increase in velocity of the flow field.
- the reactive flow under consideration based on the model assumption is a destructive reaction
- convective heat transfer is seen to decline the chemical species distributions
- Skin-Friction is a resistant force exerted on an object passing through the fluid.

Nomenclature

y	flow axis	Dimensionless group
u, v	Velocity component along x and y-axis	Bi
T	Temperature field	θ
C	Species concentration field	ϕ
g	gravitational acceleration	Gr_c
B_0	Magnetic field of uniform strength	Gr_t
T_w	surface temperature	N
T_∞	ambient temperature	λ
C_w	surface concentration	α
C_∞	ambient concentration	Nu
β_t	Volumetric coefficient of thermal expansion	Sh
β_c	Volumetric coefficient of mass expansion	H
k	thermal conductivity	Sr
c_p	specific heat capacity at constant pressure	Ec
D	Molecular diffusivity	λ
U_∞	ambient velocity	β
Q	Heat source/sink parameter	D_B

L_1	Slip velocity	h	plate heat transfer coefficient
k_r	Binary chemical reaction parameter	Pr	Prandtl number
R_G	Universal gas constant	Sc	Schmidt number
Ea	Activation Energy	Subscript	
Greek Symbol		∞	ambient condition
ρ	fluid density	w	wall condition
σ	Electrical conductivity		
μ	Fluid viscosity		$0 < \epsilon \ll 1$

Appendix

$$m = \frac{1}{2} \left(Prv_0 + \sqrt{Pr^2 v_0^2 - 4Pr\beta} \right), n = \frac{1}{2} \left(v_0 + \sqrt{v_0^2 - 4H} \right)$$

$$a_1 = \frac{Bi}{Bi + m}, a_2 = -\frac{Srma_1}{Scv_0}, a_3 = \frac{Grta_1}{-m^2 + mv_0 + H}, a_4 = \frac{Grca_2}{(-Sc^2 + Sc)v_0^2 + H}$$

$$a_5 = -\frac{ScL_0 a_4 v_0 + mL_0 a_3 + a_3 + a_4}{nL_0 + 1}, a_7 = -\frac{Eca_3^2 m^2}{-2Prmv_0 + Pr\beta + 4m^2}$$

$$a_6 = -\left((Bi + 2m)a_7 + (Scv_0 + Bi + m)a_8 + (Bi + m + n)a_9 + (2Scv_0 + Bi)(a_{10} + a_{12}) + (Scv_0 + Bi + n)a_{11} \right) / (Bi + m)$$

$$a_8 = \frac{-2\delta a_3 m a_4 Scv_0}{(Scv_0 + m)^2 - Prv_0(Scv_0 + m) + Pr\beta'}$$

$$a_9 = \frac{-2Eca_3 m a_5 n}{(m + n)^2 - Prv_0(m + n) + Pr\beta'}, a_{10} = \frac{-Eca_4^2 Sc^2 v_0^2}{-2PrScv_0^2 + 4Sc^2 v_0^2 + Pr\beta'}$$

$$a_{11} = \frac{-2Eca_4 Scv_0 a_5 n}{(-Scv_0 - n)^2 + Prv_0(-Scv_0 - n) + Pr\beta'}$$

$$a_{12} = -\frac{Eca_5^2 n^2}{-2PrScv_0^2 + 4Sc^2 v_0^2 + Pr\beta'}$$

$$a_{13} = \frac{Sr(3ma_7 + (Scv_0 + m)a_8 + (m + n)a_9 - 2Sca_{10}v_0) - \frac{\lambda a_2 a_1^r}{m} \left(\frac{a_1^2}{2(r+2)} + \frac{a_1}{r+1} + \frac{1}{r} \right)}{}$$

$$a_{14} = -\frac{1}{2} \frac{\lambda a_1^3 a_2}{m(r+2)(Scv_0 + mr + 2m)}$$

$$a_{15} = -\frac{\lambda a_1^2 a_2}{m(r+1)(Scv_0 + mr + m)}, a_{16} = -\frac{\lambda a_2 a_1^2}{mr(Scv_0 + mr)}$$

$$a_{17} = -\frac{a_{13}}{Scv_0}, a_{19} = -\frac{Grta_6}{m^2 - mv_0 - H}$$

$$a_{20} = -\frac{Grta_7}{4m^2 - 2mv_0 - H}, a_{21} = -\frac{Grta_8}{(-Scv_0 - m)^2 + v_0(-Scv_0 - m) - H}$$

$$a_{22} = -\frac{Grta_9}{(-m - n)^2 + v_0(-m - n) - H}, a_{23} = -\frac{Grta_{10} + a_{12}}{4Sc^2 v_0^2 - 2Scv_0^2 - H}$$

$$a_{24} = -\frac{Grta_{11}}{(-Scv_0 - n)^2 + v_0(-Scv_0 - n) - H}$$

$$a_{26} := -\frac{Grca_{14}}{(-Scv_0 - m(r+2))^2 + v_0(-Scv_0 - m(r+2)) - H'}$$

$$a_{27} := -\frac{Grca_{15}}{(-Scv_0 - m(r+1))^2 + v_0(-Scv_0 - m(r+1)) - H'}$$

$$a_{28} := -\frac{Grca_{16}}{(Scv_0 + mr)^2 - v_0(Scv_0 + mr) - H'}, a_{29} := -\frac{Grca_{17}}{Sc^2v_0^2 - Scv_0^2 - H'}$$

$$a_{18} := mL_0(a_{19} + 2a_{20} + v_0a_{21} + a_{22} + (r+2)a_{26} + (r+1)a_{27} + ra_{28}) + nL_0(a_{22} + a_{24}) + a_{19} + a_{20} + a_{22} + ScL_0v_0a_{23} + (ScL_0v_0 + 1)a_{24} + (ScL_0v_0 + 1)(a_{26} + a_{27} + a_{28} + a_{29} + a_{21} + a_{23}).$$

Contribution of Author: Each author made an equal contribution.

Conflict of Interest: According to the authors, there is no conflict of interest.

Acknowledgements: The management of Covenant University is appreciated and thanked by the writers for providing the conducive environment and research facilities. We also appreciate the anonymous referees' helpful comments, which helped to improve the final product.

REFERENCES

- [1] Chamkha A.J. (2003). MHD flow of uniformly stretched vertical permeable surface in the presence of heat generation/absorption and chemical reaction, *Int. Comm. Heat Mass Transfer* 30, pp 413 – 422.
- [2] Sajid, M., & Hayat, T. (2008). Influence of thermal radiation on the boundary layer flow due to an exponentially stretching sheet. *International Communications in Heat and Mass Transfer*, 35(3), 347–356.
- [3] Aliakbar, V., Alizadeh-Pahlavan, A., & Sadeghy, K. (2009). The influence of thermal radiation on MHD flow of Maxwellian fluids above stretching sheets. *Commun. Nonlinear Science Numerical Simulation*, 14, 779–794.
- [4] Siddheshwar, P. G., & Mahabaleswar, U. S. (2005). Effects of radiation and heat source on MHD flow of a viscoelastic liquid and heat transfer over a stretching sheet. *International Journal of Non-Linear Mechanics*, 40(6), 807–820.
- [5] Makinde, O. D., & Sibanda, P. (2008). Magnetohydrodynamic Mixed-Convective Flow and Heat and Mass Transfer Past a Vertical Plate in a Porous Medium With Constant Wall Suction. *Journal of Heat Transfer*, 130(11).
- [6] Chamkha, A. J., & Aly, A. M. (2010). Mhd Free Convection Flow Of A Nanofluid Past A Vertical Plate In The Presence Of Heat Generation Or Absorption Effects. *Chemical Engineering Communications*, 198(3), 425–441.
- [7] Aziz, A., & Khan, W. A. (2012). Natural convective boundary layer flow of a nanofluid past a convectively heated vertical plate. *International Journal of Thermal Sciences*, 52, 83–90.
- [8] Uddin, M. J., Khan, W. A., & Ismail, A. I. (2012). MHD Free Convective Boundary Layer Flow of a Nanofluid past a Flat Vertical Plate with Newtonian Heating Boundary Condition. *PLoS ONE*, 7(11), 49499. <https://doi.org/10.1371/journal.pone.0049499>
- [9] Samad, M. A., & Mansur-Rahman, M. (1970). Thermal Radiation Interaction with Unsteady MHD Flow Past a Vertical Porous Plate Immersed in a Porous Medium. *Journal of Naval Architecture and Marine Engineering*, 3(1), 7–14.
- [10] Hossain, Md.Anwar, & Munir, M. S. (2000). Mixed convection flow from a vertical flat plate with temperature dependent viscosity. *International Journal of Thermal Sciences*, 39(2), 173–183.
- [11] Fang, T. (2004). Influences of fluid property variation on the boundary layers of a stretching surface. *Acta Mechanica*, 171(1–2).
- [12] Mahmoud, M. A. A. (2007). Variable viscosity Effects on hydromagnetic boundary layer flow along a continuously moving vertical plate in the presence of radiation. *Applied Mathematical Sciences*, 1(17), 799–814.

- [13] Hossain, M.Anwar, Khanafer, K., & Vafai, K. (2001). The effect of radiation on free convection flow of fluid with variable viscosity from a porous vertical plate. *International Journal of Thermal Sciences*, 40(2), 115–124.
- [14] Poornima, T., & N.B., R. (2013). Radiation effects on MHD free convective boundary layer flow of nanofluids over a nonlinear stretching sheet. *Advances in Applied Science Research*, 4(2), 190–202.
- [15] Kandasamy, R., Muhaimin, I., & Mohamad, R. (2013). Thermophoresis and Brownian motion effects on MHD boundary-layer flow of a nanofluid in the presence of thermal stratification due to solar radiation. *International Journal of Mechanical Sciences*, 70, 146–154.
- [16] Ayeni, R. O., Okedoye, A. M., Popoola, A. O. and Ayodele, T. O (2005). Effect of radiation on the critical Frank-kamenestkii parameter of thermal ignition in a combustible gas containing fuel droplets. *Journal of Nigerian Association of Mathematical Physics*. 9: 17-23.
- [17] Mohammad Omidpanaha, Seyed Ali Agha Mirjalily ,b, Hadi Kargarsharifabad, Shahin shoeibi (2021) Numerical Simulation of Combined Transient Natural Convection and Volumetric Radiation inside Hollow Bricks. *Journal of Heat and Mass Transfer Research* 8 (2021) 151- 162.